

Accuracy of the new pairing theory and its improvement

L. Y. Jia^{1,2}

¹*Department of Physics, University of Shanghai for Science and Technology, Shanghai 200093, P. R. China*

²*Department of Physics, Hebei Normal University, Shijiazhuang, Hebei 050024, P. R. China*

(Dated: July 27, 2021)

Recently I proposed [1] a new method for solving the pairing Hamiltonian with the pair-condensate wavefunction ansatz based on the Heisenberg equations of motion for the density matrix operators. In this work an improved version is given by deriving the relevant equations more carefully. I evaluate both versions in a large ensemble with random interactions, and the accuracy of the methods is given statistically in terms of root-mean-square derivations from the exact results. The widely used variational calculation is also done and the results and computing-time costs are compared.

PACS numbers: 21.60.Ev, 21.10.Re,
Keywords:

I. INTRODUCTION

Pairing correlation has long been recognized in nuclei [2] and influences all the properties of the latter, such as mass, gap of excitation energy, and moment of inertia [3]. In general, any mean-field treatment of the nuclei needs to account it somehow to get reasonable results. Among the methods [4] the most popular one may be the Bardeen-Cooper-Schrieffer (BCS) theory [5], or its advanced version the Hartree-Fock-Bogoliubov (HFB) theory [3], where pairing correlation is considered by introducing quasi-particles and writing the ground state as a vacuum of the latter. But there are disadvantages of breaking the exact particle number and need for a unphysical minimum pairing strength [6, 7].

A common improvement is to use the pair-condensate [Eq. (1), the BCS wavefunction projected onto good particle number] as the ground state wavefunction [8]. Usually the criteria to determine the variational parameters is minimizing the energy in the variation principle (variation after projection BCS) [8–13]. In Ref. [1] I proposed a new criteria based on the Heisenberg equations of motion (EOM) for density matrix operators, as the lowest-order (mean-field) results of the generalized density matrix (GDM) formalism [14–20]. The method was applied to the calcium isotopes with the well known FPD6 interaction [21].

In this work I give an improved version of the method. In Ref. [1] the relevant equations are derived assuming that neighboring even-even nuclei have the same Hartree-Fock (HF) single-particle energies and occupation numbers; here I do it more carefully allowing the latters to be different. To see the validity of the approaches, both versions are applied to a large ensemble with 1000 examples and random interactions; the results are good in almost all the examples. I also compare the results and necessary computing-time costs with those of the variation principle. In Sec. II I derive the improved version of the GDM pairing theory. Then in Sec. III the approaches are evaluated in the large random ensemble. Finally Sec. IV summarizes the work and discusses further directions.

II. FORMALISM

The pairing theory in Ref. [1] was derived as the lowest-order (mean-field) results of the complete GDM formalism. In fact the derivation could be simpler and more clear if we focus on the mean fields and do not introduce collective (quadrupole) phonons. Also, in Ref. [1] I made the assumption that neighboring even-even nuclei have the same HF single-particle energies and occupation numbers. Below I derive an improved version of the pairing theory abandoning the above assumption.

As before, the ground state of the $2N$ -particle system is assumed to be an N -pair condensate,

$$|\phi_N\rangle = \frac{1}{\sqrt{\chi_N}}(P^\dagger)^N|0\rangle, \quad (1)$$

where χ_N is the normalization factor, and P^\dagger is the pair creation operator

$$P^\dagger = \frac{1}{2} \sum_1 v_1 a_1^\dagger a_{\bar{1}}^\dagger. \quad (2)$$

In Eq. (2) the summation runs over the entire single-particle space. $|\bar{1}\rangle$ is the time-reversed level of the single-particle level $|1\rangle$. The pair structure v_1 are parameters to be determined by the theory.

With the antisymmetrized fermionic Hamiltonian

$$H = \sum_{12} \epsilon_{12} a_1^\dagger a_2 + \frac{1}{4} \sum_{1234} V_{1234} a_1^\dagger a_2^\dagger a_3 a_4, \quad (3)$$

I calculate the exact Heisenberg equations of motion for the density matrix operators $R_{12} \equiv a_2^\dagger a_1$ and $K_{12} \equiv a_2 a_1$,

$$[R_{12}, H] = [\epsilon, R]_{12} - \frac{1}{2} \sum_{345} V_{5432} a_5^\dagger a_4^\dagger a_3 a_1 + \frac{1}{2} \sum_{345} V_{1345} a_2^\dagger a_3^\dagger a_4 a_5, \quad (4)$$

$$[K_{12}, H] = (\epsilon K)_{12} - (\epsilon K)_{21} + \frac{1}{2} \sum_{34} V_{1234} K_{43} - \frac{1}{2} \sum_{345} V_{1543} a_5^\dagger a_4 a_3 a_2 + \frac{1}{2} \sum_{345} V_{2543} a_5^\dagger a_4 a_3 a_1. \quad (5)$$

Terms on the right-hand sides of Eqs. (4) and (5) are read as matrix multiplications; for example, $[\epsilon, R]_{12} = (\epsilon R)_{12} - (R\epsilon)_{12} = \sum_3 \epsilon_{13} R_{32} - \sum_3 R_{13} \epsilon_{32}$.

On the pair condensate (1), the density matrices are “diagonal”:

$$\rho_{12}^N \equiv \langle \phi_N | a_2^\dagger a_1 | \phi_N \rangle = \delta_{12} n_1^N, \quad (6)$$

$$\kappa_{12}^N \equiv \langle \phi_{N-1} | a_2 a_1 | \phi_N \rangle = \delta_{12} s_1^N. \quad (7)$$

In practical shell-model calculations usually each single-particle level has distinct spin and parity, thus the mean fields are also “diagonal”:

$$f_{12}^N \equiv \epsilon_{12} + \sum_{34} V_{1432} \rho_{34}^N = \delta_{12} e_1^N, \quad (8)$$

$$\delta_{12}^N \equiv \frac{1}{2} \sum_{34} V_{1234} \kappa_{43}^N = \delta_{12} g_1^N. \quad (9)$$

The pairing mean field δ^N should not be mixed with the Kronecker delta δ .

Now I take matrix elements of the exact equations of motion between the pairing ground states (1): equation (4) between those of the same nuclei (“ $\langle \phi_N |$ ” and “ $| \phi_N \rangle$ ”); equation (5) between those of neighboring even-even nuclei (“ $\langle \phi_{N-1} |$ ” and “ $| \phi_N \rangle$ ”). On the left-hand side of Eq. (5) we have $\langle \phi_{N-1} | [K_{12}, H] | \phi_N \rangle = \langle \phi_{N-1} | K_{12} H | \phi_N \rangle - \langle \phi_{N-1} | H K_{12} | \phi_N \rangle \approx (E_N - E_{N-1}) \kappa_{12}^N$, where E_N and E_{N-1} are the ground state energies, $H | \phi_N \rangle \approx E_N | \phi_N \rangle$ and $H | \phi_{N-1} \rangle \approx E_{N-1} | \phi_{N-1} \rangle$. Similarly for Eq. (4) we have $\langle \phi_N | [R_{12}, H] | \phi_N \rangle \approx (E_N - E_N) \rho_{12}^N = 0$. On the right-hand sides the “two-body density matrices” are approximated in the following way:

$$\begin{aligned} \langle \phi_N | a_4^\dagger a_3^\dagger a_2 a_1 | \phi_N \rangle &\approx \langle \phi_N | a_4^\dagger a_1 | \phi_N \rangle \langle \phi_N | a_3^\dagger a_2 | \phi_N \rangle \\ &\quad - \langle \phi_N | a_4^\dagger a_2 | \phi_N \rangle \langle \phi_N | a_3^\dagger a_1 | \phi_N \rangle \\ &\quad + \langle \phi_{N-1} | a_4^\dagger a_3^\dagger | \phi_{N-1} \rangle \langle \phi_{N-1} | a_2 a_1 | \phi_N \rangle, \\ &= \rho_{14}^N \rho_{23}^N - \rho_{24}^N \rho_{13}^N + \kappa_{34}^{N\dagger} \kappa_{12}^N, \quad (10) \\ &\quad \langle \phi_{N-1} | a_4^\dagger a_3 a_2 a_1 | \phi_N \rangle \\ &\approx \langle \phi_{N-1} | a_4^\dagger a_1 | \phi_{N-1} \rangle \langle \phi_{N-1} | a_3 a_2 | \phi_N \rangle \\ &\quad - \langle \phi_{N-1} | a_4^\dagger a_2 | \phi_{N-1} \rangle \langle \phi_{N-1} | a_3 a_1 | \phi_N \rangle \\ &\quad + \langle \phi_{N-1} | a_4^\dagger a_3 | \phi_{N-1} \rangle \langle \phi_{N-1} | a_2 a_1 | \phi_N \rangle \\ &= \rho_{14}^{N-1} \kappa_{23}^N - \rho_{24}^{N-1} \kappa_{13}^N + \rho_{34}^{N-1} \kappa_{12}^N. \quad (11) \end{aligned}$$

Equations (10) and (11) would be exact if the ground states were taken as single-particle Slater determinants: the right-hand sides were just the fully contracted terms in Wick’s theorem. Here they are approximations because the ground states are taken as pair condensates (1). Finally Eqs. (4) and (5) become

$$0 = [f_N, \rho_N] - \kappa_N \delta_N^\dagger + \delta_N \kappa_N^\dagger, \quad (12)$$

$$\begin{aligned} (E_N - E_{N-1}) \kappa_N &= f_{N-1} \kappa_N + \kappa_N f_{N-1}^T \\ &\quad + \delta_N - \delta_N \rho_{N-1}^T - \rho_{N-1} \delta_N. \quad (13) \end{aligned}$$

Under the “diagonal” properties (6), (7), (8), and (9), Eq. (12) is satisfied automatically, and Eq. (13) becomes

$$E_N - E_{N-1} = 2e_1^{N-1} + g_1^N \frac{2n_1^{N-1} - 1}{s_1^N}. \quad (14)$$

Equation (14) is the main equation of the improved theory. It implies that the right-hand side is independent of the single-particle label 1, by which the parameters v_1 in Eq. (2) are fixed. The main equation of the old theory, Eq. (19) in Ref. [1], corresponds to replacing e_1^{N-1} and n_1^{N-1} by e_1^N and n_1^N . Equation (14) includes the well-known particle-particle random phase approximation [7] as its special case of $N = 1$ ($n^0 = 0$, $e^0 = \epsilon$). The normalization factor χ_N (1), occupation numbers n_1^N (6), pair-transfer amplitudes s_1^N (7), mean fields e_1^N (8) and g_1^N (9) are functions of the pair structures v_1 (2); their functional forms, as the “kinematics” of the system, have already been given in Eqs. (23) and (24) of Ref. [1] and are not repeated here.

In the next section I take the pairing Hamiltonian:

$$\epsilon_{12} = \delta_{12} \epsilon_1, \quad V_{1234} = -\delta_{2\bar{1}} \delta_{3\bar{4}} G_{13} \quad (15)$$

in Eq. (3). Consequently the mean fields (8) and (9) become

$$e_1^N = \epsilon_1 - G_{11} n_1^N, \quad g_1^N = \frac{1}{2} \sum_2 G_{12} s_2^N. \quad (16)$$

I apply both versions of the theory to a large random ensemble; for convenience I call Eq. (14) the “GDM2” pairing theory, and Eq. (19) in Ref. [1] the “GDM1” pairing theory.

III. RANDOM ENSEMBLE

The “GDM1” theory was applied in Ref. [1] to calcium isotopes with the FPD6 interaction and the results are good. Here I would like to consider both the “GDM1” and “GDM2” theories in a large ensemble with random interactions; consequently we can speak statistically the accuracy of the theories in terms of the root-mean-square derivations from the exact results. The variational calculation with the trial wavefunction (1) is also performed and the accuracy and computing-time cost are compared.

The random ensemble has 1000 examples with different parameters determined in the following way. For each example, I first pick up the single-particle levels randomly from the pool $2j = 1, 3, 5, 7, 9, 11, 13$. Each angular momentum j has a 40% probability of being selected; the selected ones (at least two) constitute the model space. Second, the single-particle energies ϵ_1 (15) are determined randomly following the uniform distribution from -10 MeV to 0. Third, I pick up the “pairing strength” G_{\max} as a random number following the uniform distribution from 0 to 2 MeV, then the pairing matrix elements G_{12} (15) are distributed uniformly from 0

to G_{\max} . Finally, the number of pairs N is determined following the uniform distribution from 1 to $\Omega - 1$, where $2\Omega = \sum_j (2j + 1)$ is the maximal particle number allowed by the model space.

I perform four sets of calculations for the ensemble: two GDM calculations ‘‘GDM1’’ and ‘‘GDM2’’, variational calculation ‘‘VAR’’, and the exact calculation. (In this work the exact calculation is done by diagonalization in spaces with fixed seniority [22, 23]. It can also be achieved by the Monte Carlo algorithm [24–26]; or the Richardson’s method in some special cases [27–29].) For the variational calculation of the pair-transfer amplitudes $s_1 = \langle \phi_{N-1} | a_1^\dagger a_1 | \phi_N \rangle$ (7), I show two sets of results. In ‘‘VAR1’’ the pair structure v_1 (2) in $|\phi_{N-1}\rangle$ and $|\phi_N\rangle$ are the same, given by minimizing $\langle \phi_N | H | \phi_N \rangle$; while in ‘‘VAR2’’ v_1 in $|\phi_{N-1}\rangle$ and $|\phi_N\rangle$ are different, given by minimizing $\langle \phi_{N-1} | H | \phi_{N-1} \rangle$ and $\langle \phi_N | H | \phi_N \rangle$, respectively.

In Figs. 1 and 2 I show the complete spectroscopic results for the ensemble. For example, in panel (a) of Fig. 1 there are 3154 points (crosses), corresponding to the 3154 single-particle levels in the 1000 examples of the ensemble. The horizontal coordinate of each point is the exact value of n_1 of the corresponding single-particle level, while the vertical coordinate is the ‘‘GDM1’’ value. Thus a perfect calculation would have all the points lying on the $y = x$ straight line. Similarly, in panels (b) and (c) of Fig. 1 the vertical coordinates are the ‘‘GDM2’’ and ‘‘VAR’’ values of n_1 , respectively. Figure 2 is plotted in the same way for the pair-transfer amplitudes s_1 . From Figs. 1 and 2 we see that the variational calculation for n_1 and the ‘‘VAR2’’ version of s_1 are generally better than the GDM ones. However, the less-careful ‘‘VAR1’’ calculation of s_1 is worse than the GDM ones. The root-mean-square (σ) derivations from the exact results are

$$\sigma_n^{\text{GDM1}} = 0.0122, \sigma_n^{\text{GDM2}} = 0.0188, \sigma_n^{\text{VAR}} = 0.0045, \quad (17)$$

on Fig. 1 and

$$\begin{aligned} \sigma_s^{\text{GDM1}} &= 0.0207, \sigma_s^{\text{GDM2}} = 0.0191, \\ \sigma_s^{\text{VAR1}} &= 0.0373, \sigma_s^{\text{VAR2}} = 0.0091, \end{aligned} \quad (18)$$

on Fig. 2. We note that on Fig. 2 there is a point much worse than others for all the calculations, so let us look at the particular example it belongs to. This example has $2N = 12$ particles on two single-particle levels with angular momenta $j = \frac{5}{2}, \frac{9}{2}$ and energies $\epsilon_{\frac{5}{2}} = -8.988$, $\epsilon_{\frac{9}{2}} = -9.390$ MeV. The pairing two-body matrix elements are $G_{\frac{5}{2}, \frac{5}{2}} = 0.4252$, $G_{\frac{9}{2}, \frac{9}{2}} = 0.0456$, and $G_{\frac{5}{2}, \frac{9}{2}} = G_{\frac{9}{2}, \frac{5}{2}} = 0.0016$ MeV. The failed point corresponds to the $j = \frac{5}{2}$ level. This example is particular in that $\epsilon_{\frac{5}{2}} - \epsilon_{\frac{9}{2}} \approx G_{\frac{5}{2}, \frac{5}{2}} \gg G_{\frac{9}{2}, \frac{9}{2}} \gg G_{\frac{5}{2}, \frac{9}{2}}$, thus there is little correlation between the two levels. I have looked at the exact wavefunction of the daughter nucleus and it is mainly $P_{\frac{5}{2}}^\dagger (P_{\frac{9}{2}}^\dagger)^4 |0\rangle$, which is not representable by Eq. (1). Without this example, the root-mean-square derivations for the pair-transfer amplitudes s_1 are

$$\sigma_s^{\text{GDM1}} = 0.0177, \sigma_s^{\text{GDM2}} = 0.0163, \sigma_s^{\text{VAR1}} = 0.0352, \text{ and } \sigma_s^{\text{VAR2}} = 0.0079.$$

The necessary formula for the GDM and variational calculations were given in Ref. [1]. In general, in large model spaces the GDM calculation costs less time than the variational one, by a factor of the number of non-degenerate single-particle levels (in order of magnitude), because the former needs to calculate only $\langle \phi_{N-1} | P_1 | \phi_N \rangle$ while the latter needs $\langle \phi_N | P_1^\dagger P_2 | \phi_N \rangle$ ($P_1^\dagger \equiv a_1^\dagger a_1^\dagger$). However, as we can see from Figs. 1 and 2 and Eqs. (17) and (18), the accuracy of the GDM method is close to that of the variational one. The reduction of time cost may be a big advantage when doing ab-initio mean-field calculations for medium and heavy nuclei, especially if we were fitting parameters of the interaction (for example the effort in developing density functionals with spectroscopic accuracy).

Next I would like to see the accuracy of the methods depending on different quantities. For this purpose I plot the root-mean-square derivations of n_1 and s_1 as functions of the single-particle angular momentum j , particle number $2N$, and pairing strength G_{\max} in Figs. 3, 4, and 5, respectively. We have the following observations: 1. From Figs. 3 and 4 we see that as a trend the GDM results improve with increasing j and N , which should be expected because the GDM formalism is a collective theory. 2. There seems to be no obvious trend with the pairing strength shown in Fig. 5. 3. On Fig. 4, the GDM2 calculation for $N = 1$, which is the particle-particle random phase approximation, is much better than the GDM1 calculation. And for small N (until $N = 6$), the GDM2 s_1 seems to be slightly better than the GDM1 s_1 . 4. On Fig. 3, the GDM2 s_1 is slightly better than the GDM1 s_1 at the smallest angular momenta $j = \frac{1}{2}$ and $\frac{3}{2}$. For these levels the difference $n_1^N - n_1^{N-1}$, which is inversely proportional to j around the Fermi surface, is largest; and the GDM2 theory with n_1^{N-1} seems to be slightly better than the GDM1 one with n_1^N . 5. The GDM1 n_1 seems to be consistently better than the GDM2 n_1 and the reason is still unclear. 6. In panel (c) of Figs. 3, 4, and 5 the worst points are at $2j = 5$, $N = 6$, and $0.5 \text{ MeV} < G_{\max} < 0.6 \text{ MeV}$, respectively; because these three sub-groups contain the ‘‘worst’’ example mentioned below Eq. (18).

At last in Fig. 6 I show the results for the ground state energy by different calculations. In panel (a) there are 1000 points (crosses), corresponding to the 1000 examples of the ensemble. The horizontal coordinate of each point is the pairing correlation energy of the corresponding example, $E_{\text{pair}} \equiv \sum_1 \epsilon_1 n_1^F - E_{\text{shell}}$, where E_{shell} is the exact ground state energy of the shell model calculation, and $n_1^F = 1$ or 0 is the occupation number of the naive Fermi distribution. The vertical coordinate shows the variational ground state energy measured from the exact one, $E_{\text{var}} = \langle \phi_N^{\text{var}} | H | \phi_N^{\text{var}} \rangle - E_{\text{shell}}$, where $|\phi_N^{\text{var}}\rangle$ is the pair condensate (1) with its pair structure v_1 (2) determined by the variation principle. Similarly for panels (b) and (c), but the vertical co-

ordinates are the ground state energies of the GDM1 and GDM2 calculations, respectively, measured from the exact one ($E_{\text{GDM1}} = \langle \phi_N^{\text{GDM1}} | H | \phi_N^{\text{GDM1}} \rangle - E_{\text{shell}}$ and $E_{\text{GDM2}} = \langle \phi_N^{\text{GDM2}} | H | \phi_N^{\text{GDM2}} \rangle - E_{\text{shell}}$). We see that all the three calculations give good ground state energies: the errors are small relative to the pairing correlation energy. The average values are $\bar{E}_{\text{var}} = 0.045$, $\bar{E}_{\text{GDM1}} = 0.061$, $\bar{E}_{\text{GDM2}} = 0.070$, and $\bar{E}_{\text{pair}} = 13.64$ MeV. It is well known that the variational calculation finds the best and lowest ground state energy for a set of restricted wavefunctions of the form (1). However, from the above average values we see that the energies of the GDM wavefunctions $|\phi_N^{\text{GDM1}}\rangle$ and $|\phi_N^{\text{GDM2}}\rangle$ are close to the variational minimum $\langle \phi_N^{\text{var}} | H | \phi_N^{\text{var}} \rangle$.

IV. SUMMARY

In summary, I derive a physically improved version of the GDM pairing theory proposed in Ref. [1]. Both versions are checked in a large random ensemble, and the accuracy is given statistically in terms of root-mean-square derivations from the exact results. Consequently, we could consider the theories to be correct and apply them with confidence to realistic systems.

Based on the results, the GDM theories are not as accurate as (although close to) the variation principle.

However, the reduction of computing-time cost is huge for large model spaces (by a factor of the number of non-degenerate single-particle levels). This should be interesting for ab-initio mean-field calculations of medium and heavy nuclei (especially if deformed Nilsson single-particle levels were used), or the effort in fitting parameters of an interaction.

Comparing the two versions of the GDM theory, we see that in general the new one (physically more reasonable) is slightly better in calculating pair-transfer amplitudes s_1 , while the old one produces better occupation numbers n_1 and slightly better ground state energy. The reason for the latter is still unclear.

The key approximation of the current GDM methods is the ‘‘factorization’’ or ‘‘linearization’’ of the two-body density matrix on the pair condensate [Eqs. (10) and (11)]. It would be interesting to see its validity in other circumstances, in particular, whether we could use it in the variational formalism when calculating the two-body part of the average energy, which would reduce the time cost to the same level of the current GDM methods.

Support is acknowledged from the startup funding for new faculty member in University of Shanghai for Science and Technology. The numerical calculations of this work are done at the High Performance Computing Center of Michigan State University.

-
- [1] L. Y. Jia, Phys. Rev. C **88**, 044303 (2013).
 - [2] A. Bohr, B. R. Mottelson, and D. Pines, Phys. Rev. **110**, 936 (1958).
 - [3] S. T. Belyaev, K. Dan. Vidensk. Selsk. Mat. Fys. Medd. **31**, (11) (1959).
 - [4] Ricardo A Broglia, and Vladimir Zelevinsky, *Fifty Years of Nuclear BCS: Pairing in Finite Systems* (World Scientific, 2013).
 - [5] J. Bardeen, L. N. Cooper, and J. R. Schrieffer, Phys. Rev. **106**, 162 (1957); Phys. Rev. **108**, 1175 (1957).
 - [6] A. Bohr and B. Mottelson, *Nuclear Structure* (Benjamin, New York, 1975).
 - [7] P. Ring and P. Schuck, *The Nuclear Many-Body Problem* (Springer-Verlag, Berlin, 1980).
 - [8] K. Dietrich, H. J. Mang, and J. H. Pradal, Phys. Rev. **135**, B22 (1964).
 - [9] L.M. Robledo, G.F. Bertsch, arXiv:1205.4443 [nucl-th] (2012).
 - [10] H. Flocard and N. Onishi, Annals of Physics **254**, 275 (1997).
 - [11] Fabian Braun and Jan von Delft, Phys. Rev. Lett. **81**, 4712 (1998).
 - [12] J. Dukelsky and G. Sierra, Phys. Rev. B **61**, 12302 (2000).
 - [13] Jan von Delft and D.C. Ralph, Physics Reports **345**, 61 (2001).
 - [14] A. Kerman and A. Klein, Phys. Rev. **132**, 1326 (1963).
 - [15] S.T. Belyaev and V.G. Zelevinsky, Yad. Fiz. **11**, 741 (1970) [Sov. J. Nucl. Phys. **11**, 416 (1970)]; Yad. Fiz. **16**, 1195 (1972) [Sov. J. Nucl. Phys. **16**, 657 (1973)]; Yad. Fiz. **17**, 525 (1973) [Sov. J. Nucl. Phys. **17**, 269 (1973)].
 - [16] V.G. Zelevinsky, Prog. Theor. Phys. Suppl. **74-75**, 251 (1983).
 - [17] M.I. Shtokman, Yad. Fiz. **22**, 479 (1975) [Sov. J. Nucl. Phys. **22**, 247 (1976)].
 - [18] L. Y. Jia, Phys. Rev. C **84**, 024318 (2011).
 - [19] L. Y. Jia, and V. G. Zelevinsky, Phys. Rev. C **84**, 064311 (2011).
 - [20] L. Y. Jia, and V. G. Zelevinsky, Phys. Rev. C **86**, 014315 (2012).
 - [21] W.A. Richter, M.G. Van Der Merwe, R.E. Julies, and B.A. Brown, Nucl. Phys. **A523**, 325 (1991).
 - [22] H. Molique and J. Dudek, Phys. Rev. C **56**, 1795 (1997).
 - [23] V. Zelevinsky and A. Volya, Nucl. Phys. **A752**, 325 (2005).
 - [24] N. Cerf and O. Martin, Phys. Rev. C **47**, 2610 (1993);
 - [25] N. Cerf, Nucl. Phys. **A564**, 383 (1993).
 - [26] Abhishek Mukherjee, Y. Alhassid, and G. F. Bertsch, Phys. Rev. C **83**, 014319 (2011).
 - [27] R. W. Richardson, Phys. Lett. **3**, 277 (1963); Phys. Rev. **141**, 949 (1966).
 - [28] J. Dukelsky, S. Pittel, and G. Sierra, Rev. Mod. Phys. **76**, 643 (2004).
 - [29] J. Dukelsky, S. Pittel, arXiv:1204.2950 [nucl-th] (2012).

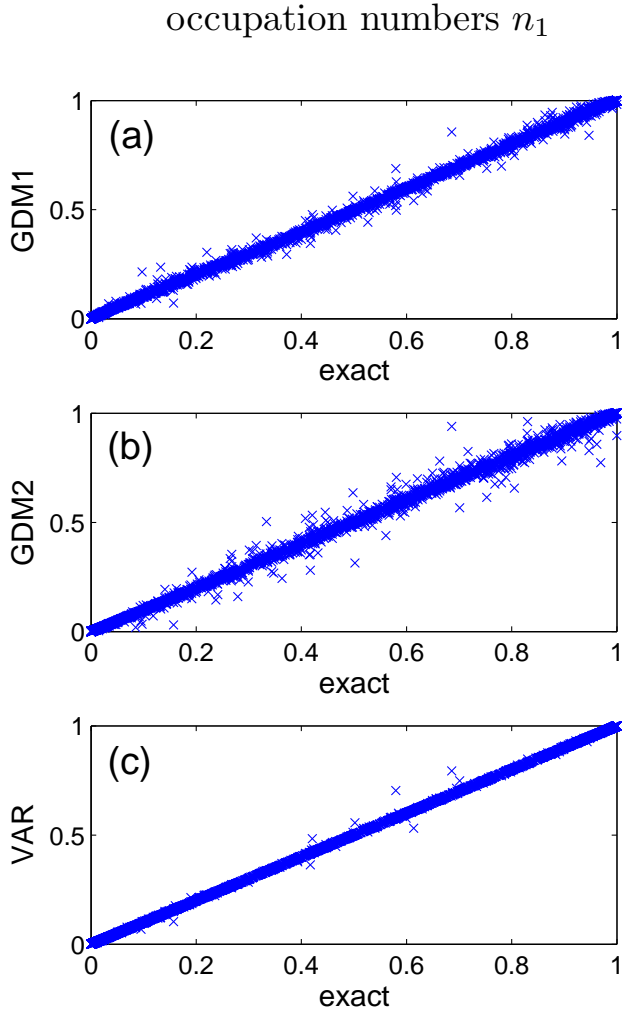


FIG. 1: (Color online) Occupation numbers n_1 of all the 3154 single-particle levels in the ensemble by different calculations. In panel (a), the single-particle levels and the points are in one-to-one correspondence, with the horizontal coordinate of the point being the exact n_1 and the vertical coordinate being the GDM1 n_1 . Similarly for panels (b) and (c), but the vertical coordinates are n_1 of the GDM2 and the variational calculations, respectively. See text for details.

pair-transfer amplitudes s_1

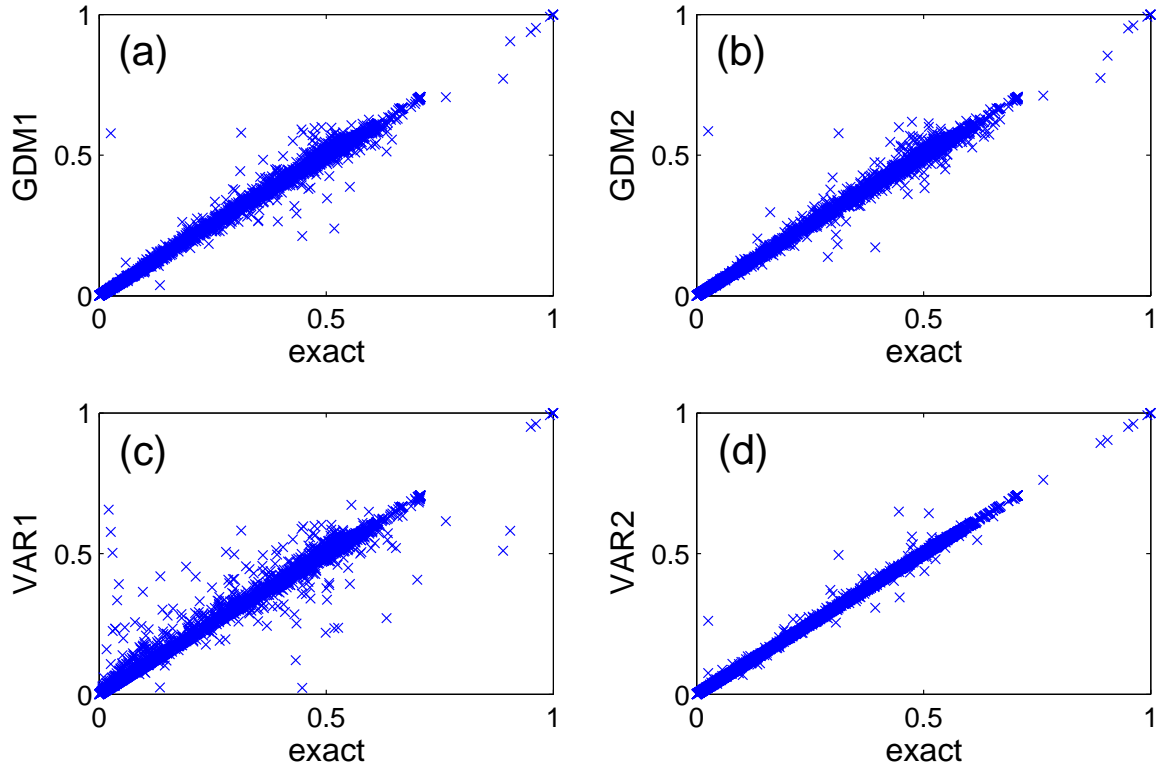


FIG. 2: (Color online) Pair-transfer amplitudes s_1 of all the 3154 single-particle levels in the ensemble by different calculations. The points are plotted in the same way as those in Fig. (1), but for the transfer amplitudes s_1 . Panels (c) and (d) plot two sets of variational calculations (see text for details).

single-particle-level groups with different j

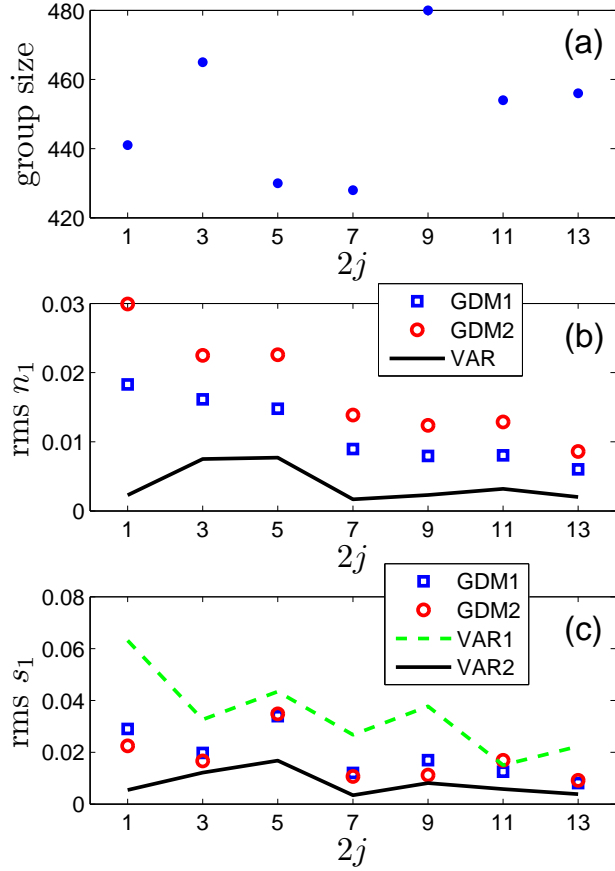


FIG. 3: (Color online) Results of different calculations grouped by the single-particle-level angular momentum j . I divide all the 3154 single-particle levels in the ensemble into different groups according to their angular momentum j , and panel (a) plots the group sizes. Panel (b) plots the root-mean-square derivations from the exact results of the occupation numbers n_1 by different calculations (GDM1, GDM2, VAR) within each j group. Similarly, panel (c) plots the root-mean-square derivations of the pair-transfer amplitudes s_1 by four sets of calculations (GDM1, GDM2, VAR1, VAR2). See text for details.

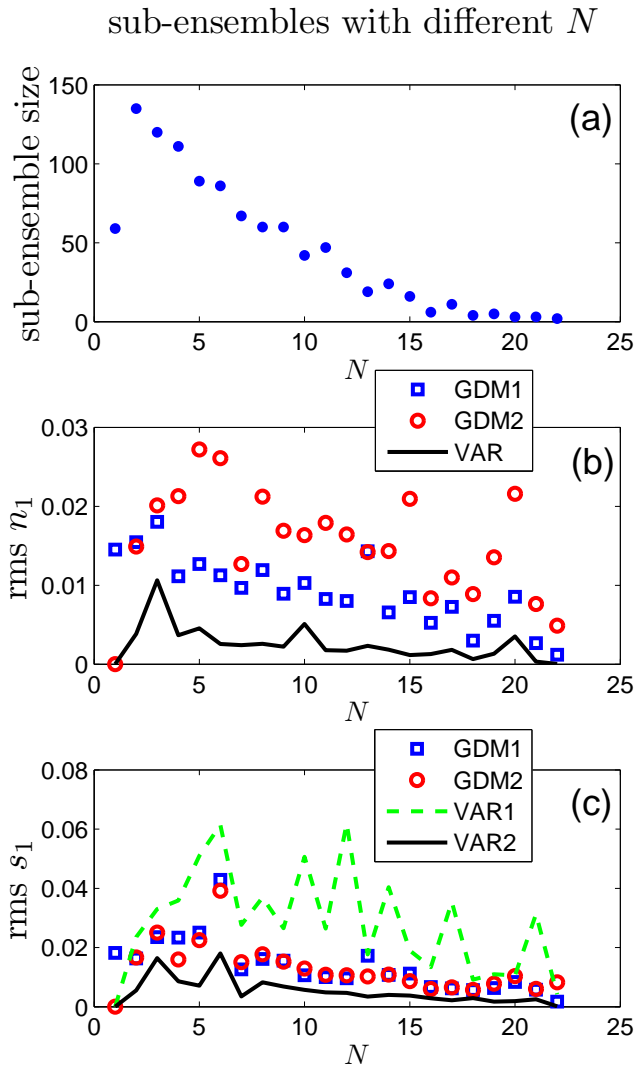


FIG. 4: (Color online) Results of different calculations in sub-ensembles divided by the particle number $2N$. The 1000 examples in the ensemble are divided into sub-ensembles according to their particle number $2N$, and panel (a) plots the sizes of the sub-ensembles. Panels (b) and (c) plot the root-mean-square derivations by different calculations of the occupation numbers n_1 and pair-transfer amplitudes s_1 within each N sub-ensemble. See text for details.

sub-ensembles with different pairing strength

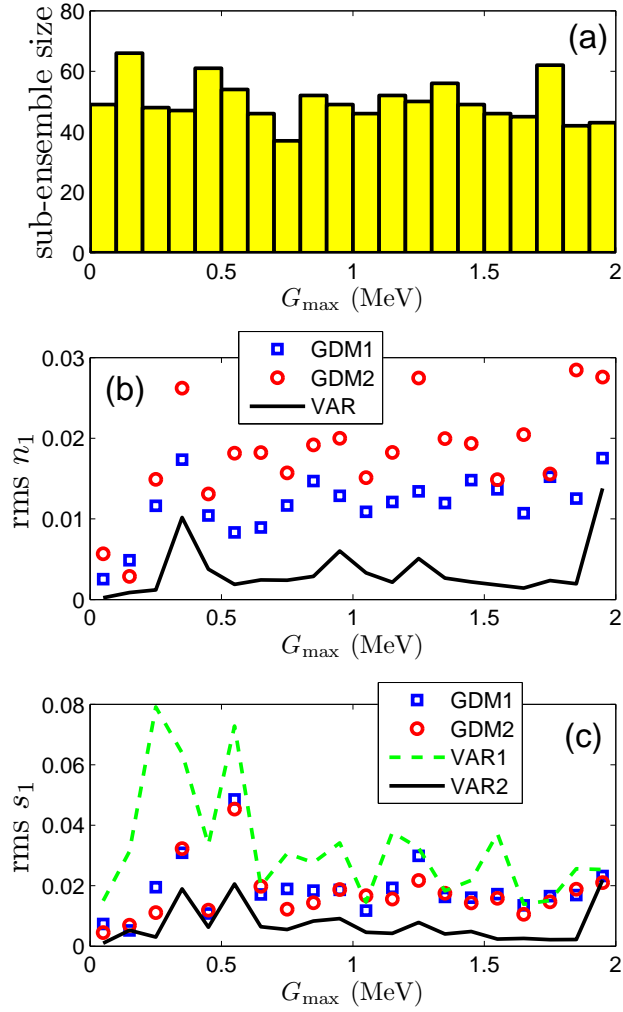


FIG. 5: (Color online) Results of different calculations in sub-ensembles divided by the pairing strength G_{\max} . The 1000 examples in the ensemble are divided into 20 sub-ensembles according to their pairing strength G_{\max} , and panel (a) plots the sizes of the sub-ensembles. Panels (b) and (c) plot the root-mean-square deviations by different calculations of the occupation numbers n_1 and pair-transfer amplitudes s_1 within each sub-ensemble. See text for details.

ground state energies

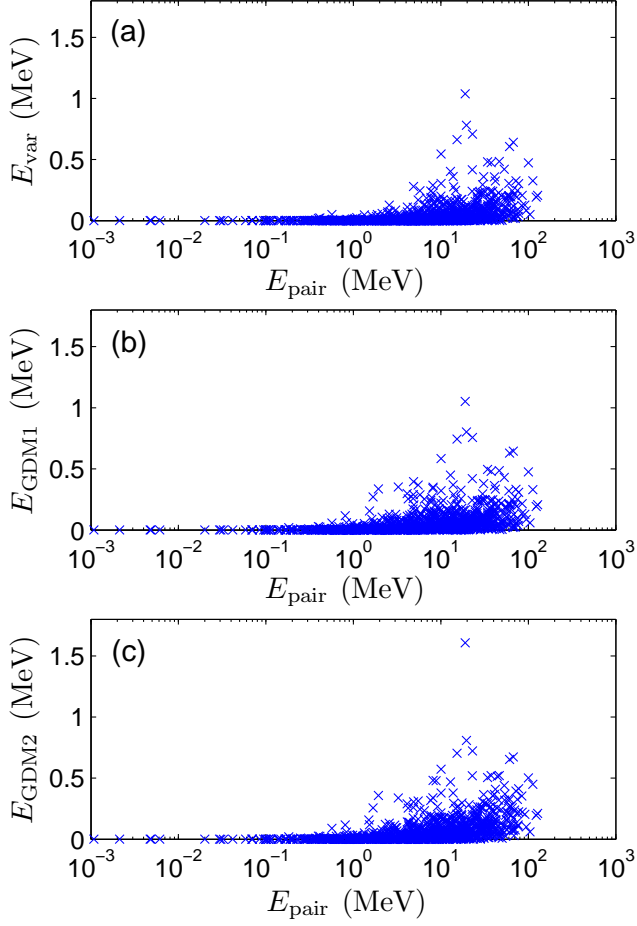


FIG. 6: (Color online) Ground state energies of all the 1000 examples by different calculations. In panel (a), the examples and the points are in one-to-one correspondence, with the horizontal coordinate of the point being the pairing correlation energy E_{pair} , and the vertical coordinate being the variational ground state energy E_{var} measured from the exact ground state energy. Similarly for panels (b) and (c), but the vertical coordinates are ground state energies by the GDM1 and GDM2 calculations, respectively, measured from the exact ground state energy. See text for details.